Silicon (2020) 12:1925–1941
https://doi.org/10.1007/s12633-019-00291-6

ORIGINAL PAPER

# Effect of Nanoclay/Nanosilica on the Mechanical Properties, Abrasion and Swelling Resistance of EPDM/SBR Composites

S. Vishvanathperumal[1] · G. Anand[2]

Received: 24 May 2019 / Accepted: 9 October 2019 / Published online: 21 November 2019


## Abstract

In this research work, ethylene-propylene-diene monomer (EPDM)/styrene butadiene rubber (SBR) hybrid composites reinforced with nanoclay (NC) and nanosilica (NS) were prepared and investigated. The synergistic effect of NC and NS on the mechanical properties of the EPDM/SBR hybrid composites was examined. Three different crosslinking systems were used, namely: sulphur, dicumyl peroxide and the mixed system consisting of sulphur and peroxide in this research work. The tensile strength, elongation at break, 100% modulus, tear strength, hardness, rebound resilience, abrasion resistance, compression set, swelling resistance and microstructure of the EPDM/SBR hybrid composites were evaluated. The concentration nanosilica along with nanoclay plays a most vital role in the micro-structural, mechanical and other properties of the nanocomposites. From the study, it was clear that the nanocomposites containing 7.5 parts per hundred rubber (phr) of nanoclay and 4 phr of nanosilica shows a maximum mechanical properties along with its abrasion and swelling resistance characteristics. In particular, the sulphur cured EPDM/SBR hybrid composites containing nanoclay and nanosilica results in best mechanical properties and abrasion resistance.

**Keywords** Nanoclay · Nanosilica · Nanocomposites · Mechanical properties · Swelling resistance

## 1 Introduction

SBR was the first developed low cost synthetic rubber used in manufacturing industries. SBR despite having good mechanical and abrasive properties, they are too sensitive towards the environmental factors such as moisture, ozone, light, and heat. This was due to the presence of double bond present in the polymeric chain which can be surmount by blending it with well saturated elastomers like EPDM. EPDM was a special type of rubber used in variety of industrial applications in day to day life. EPDM rubbers exhibits a superior oxidative and heat resistant characteristics due to the substantial absence of unsaturated chain in polymeric backbone [1, 2]. Carbon black (CB) and amorphous silica was used to improve mechanical properties of rubber composites, and have been used as an important reinforcing agent in the rubber industries in the recent decades [3–5]. Later, other reinforcing materials such as nanoclay [6–12], nanosilica [13], calcium carbonate [14] and carbon nanotubes [15] have received a great deal of attention in rubber industries due to their unique structures and their easy accessibility in comparison with other reinforcing nano-particles. The use of nanoclay in the EPDM rubber [16, 17], SBR [18–20] and EPDM/SBR [21, 22] has been reported by many researchers in recent decades.

The waste materials such as groundnut shell, rice husk (RH), sugarcane bagasse and bamboo leaves are considered as a natural source of silica. These waste materials are burnt and the ash obtained from it are rich in silica and carbon content, which has no exploitation yet. Rice husk ash was the material that consists of about 90–98% of silica after the complete combustion of it. Extraction of silica from rice husk was an emerging trend in the existing research field. Enormous amount of rice husk are treated as the waste materials and are disposed as the landfill. But burning of rice husk materials will lead to stern ecological pollutions. The suspended ash particles in the atmosphere lead to respiratory problems in human beings [23]. The commonly extracted silica (tetra ethyl orthosilicate) was more expensive, and hence

✉ G. Anand
anand.12ng@gmail.com; anand.g@pec.edu

[1] Department of Mechanical Engineering, Adhiparasakthi Engineering College, Melmaruvathur, India

[2] Department of Mechanical Engineering, MVJ College of Engineering, Bangalore, India

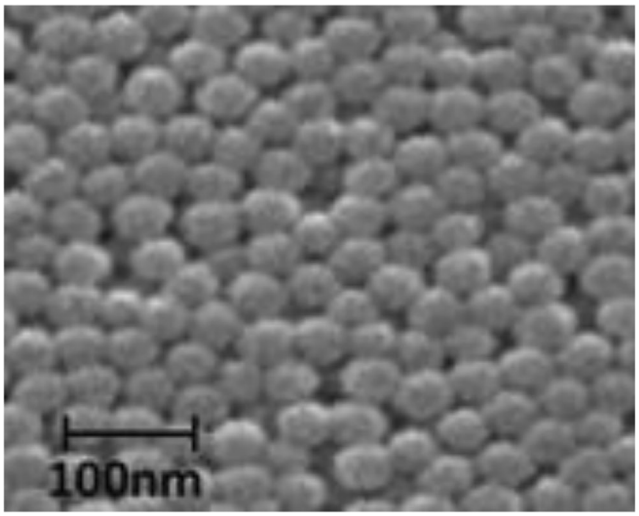


**Fig. 1** SEM images prepared of nanosilica

rice husk ash (having adequate silica) can be used as an alternative source [24, 25].

A wide-ranging of particulates was used as the reinforcing materials in the rubber industry [26]. Reinforcements are generally used to enhance the strength, modulus, hardness and abrasion resistance of the rubber composite [27]. The idea of combining EPDM with SBR was definitely not a new one. But these rubber blends are capable of forming a link between dissimilar rubbers to produce a compatible blend. The rubber blends thus produces highest tensile strength, tear strength and abrasion resistance when the ratio of blends was 80/20 for EPDM/SBR [28]. The maximum kinetic result with worthy control over molecular weight with fine molecular distribution was detected in the Cloisite 30B (compare to Closite $Na^+$ and Cloisite 15A) [29]. The effect of Cloisite 30B loading on the structure (x-ray diffraction, scanning electron microscopy and transmission electron microscopy) and properties (mechanical, rheological and thermal) of the poly(ethyl acrylate) nanocomposites by in situ polymerization and thus ensures a good compatible between polymer and Cloisite 30B [30]. The EPDM/SBR blends containing 7.5 phr of nanoclay (Cloisite 30B) shows a better mechanical properties, compression set, rebound resilience, swelling and abrasion resistance [31]. Nanosilica was generally used to improve the physical, mechanical and thermal properties of the rubber and its composite compounds [32, 33]. This was due to the high surface area property of the nanosilica. The load applied in the composite rubber was transferred from the polymer (rubber) matrix to the reinforcement (nanosilica) particles [34]. It was difficult to manufacture a rubber composite to the industrial application by reinforcing single filler in it. Generally in industries there was the demand for materials having superior properties with respect to its weight ratio, thus the hybrid composites comes

**Table 1** Formulation for EPDM/SBR/NC/NS rubber blends

| Cross-linking system types | Sample code | Compounds (phr) | | | | | | | | | | |
|---|---|---|---|---|---|---|---|---|---|---|---|---|
| | | EPDM | SBR | NC | NS | Si-69 | Zinc oxide | Stearic acid | MBTS | TMTD | S | DCP |
| Sulphur system | $S_0$ | 80 | 20 | 7.5 | 0 | – | 4 | 1.5 | 1.2 | 1 | 2.5 | – |
| | $S_1$ | 80 | 20 | 7.5 | 1 | 3 | 4 | 1.5 | 1.2 | 1 | 2.5 | – |
| | $S_2$ | 80 | 20 | 7.5 | 2 | 3 | 4 | 1.5 | 1.2 | 1 | 2.5 | – |
| | $S_3$ | 80 | 20 | 7.5 | 3 | 3 | 4 | 1.5 | 1.2 | 1 | 2.5 | – |
| | $S_4$ | 80 | 20 | 7.5 | 4 | 3 | 4 | 1.5 | 1.2 | 1 | 2.5 | – |
| | $S_5$ | 80 | 20 | 7.5 | 5 | 3 | 4 | 1.5 | 1.2 | 1 | 2.5 | – |
| | $S_6$ | 80 | 20 | 7.5 | 6 | 3 | 4 | 1.5 | 1.2 | 1 | 2.5 | – |
| Peroxide system | $P_0$ | 80 | 20 | 7.5 | 0 | – | – | – | – | – | – | 4 |
| | $P_1$ | 80 | 20 | 7.5 | 1 | 3 | – | – | – | – | – | 4 |
| | $P_2$ | 80 | 20 | 7.5 | 2 | 3 | – | – | – | – | – | 4 |
| | $P_3$ | 80 | 20 | 7.5 | 3 | 3 | – | – | – | – | – | 4 |
| | $P_4$ | 80 | 20 | 7.5 | 4 | 3 | – | – | – | – | – | 4 |
| | $P_5$ | 80 | 20 | 7.5 | 5 | 3 | – | – | – | – | – | 4 |
| | $P_6$ | 80 | 20 | 7.5 | 6 | 3 | – | – | – | – | – | 4 |
| Mixed system | $M_0$ | 80 | 20 | 7.5 | 0 | – | 4 | 1.5 | 1.2 | 1 | 2.5 | 4 |
| | $M_1$ | 80 | 20 | 7.5 | 1 | 3 | 4 | 1.5 | 1.2 | 1 | 2.5 | 4 |
| | $M_2$ | 80 | 20 | 7.5 | 2 | 3 | 4 | 1.5 | 1.2 | 1 | 2.5 | 4 |
| | $M_3$ | 80 | 20 | 7.5 | 3 | 3 | 4 | 1.5 | 1.2 | 1 | 2.5 | 4 |
| | $M_4$ | 80 | 20 | 7.5 | 4 | 3 | 4 | 1.5 | 1.2 | 1 | 2.5 | 4 |
| | $M_5$ | 80 | 20 | 7.5 | 5 | 3 | 4 | 1.5 | 1.2 | 1 | 2.5 | 4 |
| | $M_6$ | 80 | 20 | 7.5 | 6 | 3 | 4 | 1.5 | 1.2 | 1 | 2.5 | 4 |

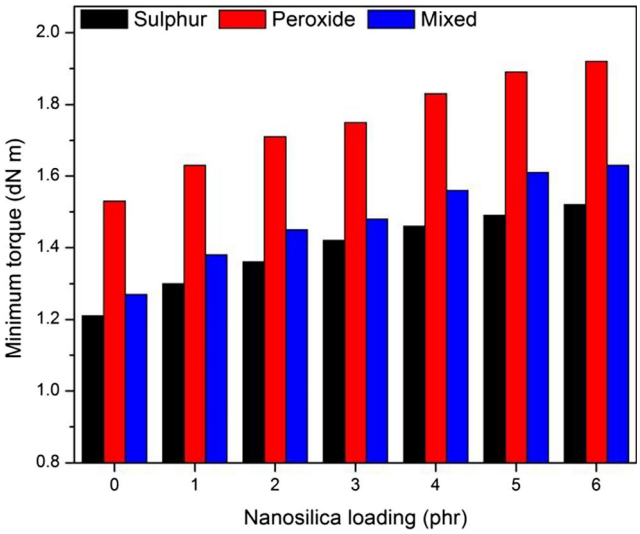


**Fig. 2** Minimum torque of EPDM/SBR-NC/NS composites

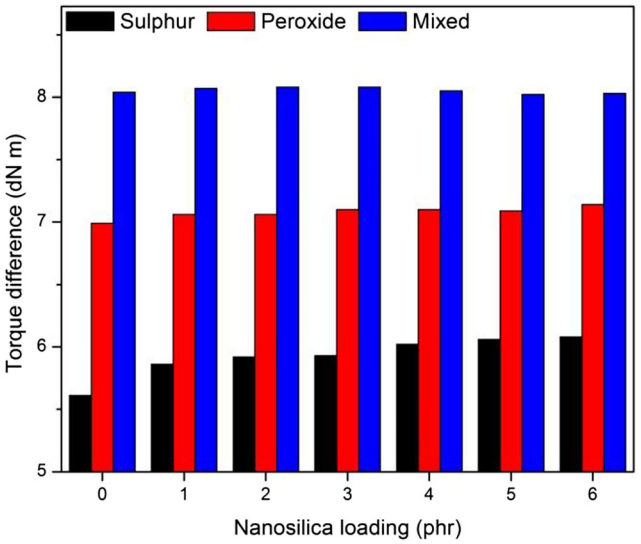


**Fig. 4** Torque difference of EPDM/SBR-NC/NS composites

into picture which has a combination of more than one fillers in it at nano scale dimension with ensures a superior properties for the fabricated composite. In the past decade, many researchers have worked in formulating newer hybrid nanocomposites with tailor made properties. The disadvantage of one filler can be overcome by the addition of another in the composite.

The nanoclay particles were alone used as the reinforcement in EPDM/SBR nanocomposites which results in improved mechanical properties, ageing, abrasion and swelling resistances as stated by Vishvanathperumal et al. [31]. In this research work, a new hybrid composite was prepared with a matrix blended with EPDM/SBR and reinforced along with different concentration of nanoclay and nanosilica particles. The silica nanoparticles used as the reinforcement in this study was extracted from the natural rice husk. The effect of reinforcement on the cure characteristics, mechanical properties, abrasion, swelling resistance, and compression set on the hybrid composites with different cross-linking systems (i.e., sulphur, peroxide and mixed system) was studied and investigated in depth in the current research.

## 2 Experimental Details

### 2.1 Materials

Ethylene-propylene-diene rubber (EPDM KEP 270), Mooney viscosity (ML (1 + 4) 125 °C) 60 M, ethylene content 68 wt.%, termonomer content (ethylidenenorbornene) 4.5%, density 0.86 g/cm$^3$ and styrene-butadiene rubber (SBR-1502), styrene content 23.5 wt.%, Mooney viscosity (ML (1 + 4) 100 °C) 52 M, density 0.93 g/cm$^3$was procured from Arihant Reclamation Private Limited, New Delhi, India.

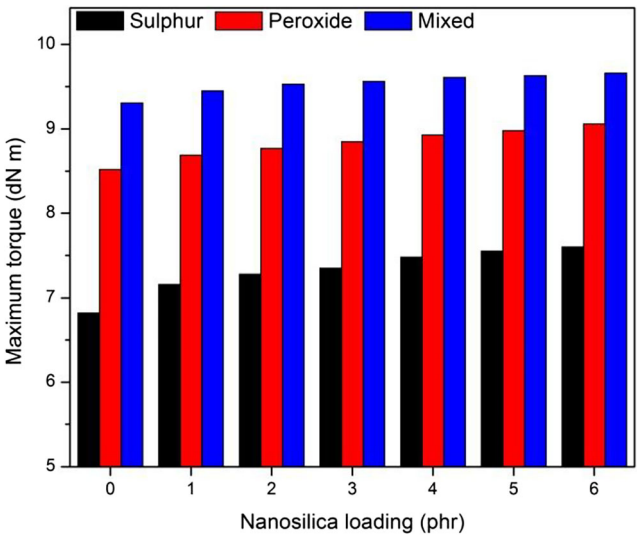


**Fig. 3** Maximum torque of EPDM/SBR-NC/NS composites

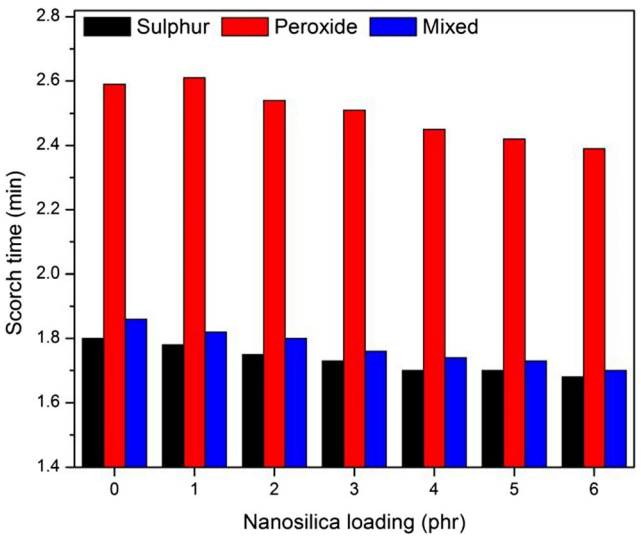


**Fig. 5** Scorch time of EPDM/SBR-NC/NS composites

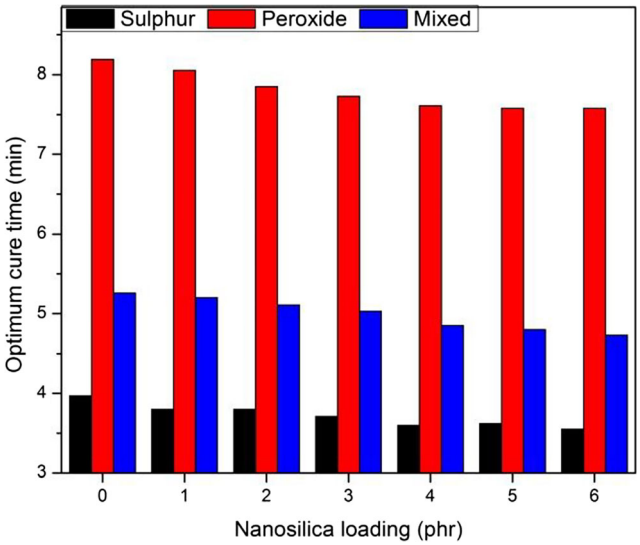


**Fig. 6** Optimum cure time of EPDM/SBR-NC/NS composites

Cloisite 30B (organo-modified layered nanosilicates), modifier concentration exchange cation exchange capacity of 90 meqv./100 g clay, methyl-tallow-bis (hydroxyethyl)-ammonium treated montmorillonite was procured from Southern Clay Products, USA. Rice husk are collected from Bahour, Puducherry, India. Nanosilica was synthesized in our laboratory by dissolution and precipitation process. Zinc oxide, stearic acid, bis (3-triethoxysilylpropyl) tetrasulphide (Si-69), mercapto benzo thiazyl disulphide (MBTS), tetra methyl thiuram disulphide (TMTD), sulphur and dicumyl peroxide of commercial grade were obtained from Vinesh Chemicals, Ambattur, Chennai, India. Benzene, toluene, xylene, mesitylene, n-pentane, n-hexane, n-heptane, n-octane, dichloromethane, chloroform and carbon tetrachloride of analytical grade of 99.95% purity was procured from Sigma Aldrich.

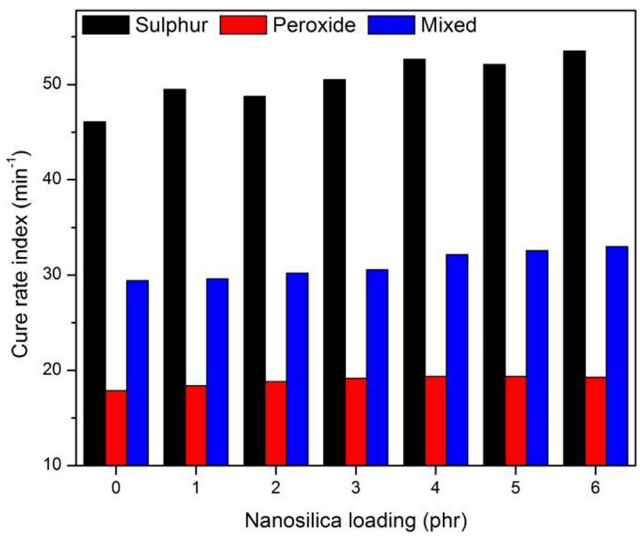


**Fig. 7** Cure rate index of EPDM/SBR-NC/NS composites

## 2.2 Preparation of Nanosilica

The moisture present in the rice husk was removed by treating it in the hot plate. Then it was heated upto 900 °C for 7 h in a furnace and the ash was collected. The ash obtained from the rice husk was used to prepare nanosilica in two stages say dissolution process and precipitation process. Initially, it was dissolved in the alkali leaching solution (made up of 1 mol of sodium hydroxide (NaOH)) to partially dissolve carbonaceous materials present in it. Thus the obtained solution of sodium silicate ($Na_2SiO_3$) was cleaned (filtered) and desiccated in the oven for 24 h at 100 °C.Then the precipitation of silica from sodium silicate ($Na_2SiO_3$) solution was treated in 6 mol of sulphuric acid ($H_2SO_4$) at the 7 pH for 24 h. The precipitate of silica was centrifuged, washed in hot water and dried at 80 °C for 24 h [35]. From scanning electron microscope (SEM) analysis it was clear that the nanosilica with a particle size of 30- 50 nm in diameter was prepared which was almost in spherical in shape and was shown in Fig. 1.

*Dissolution Process*

$$SiO_2 + 2NaOH \longrightarrow Na_2SiO_3 + H_2O$$

*Precipitation Process*

$$Na_2SiO_3 + H_2SO_4 \longrightarrow SiO_2 + Na_2SO_4 + H_2O$$

## 2.3 Preparation of Nanocomposites

The nanocomposites with different concentration were prepared in two roll mixing mill with an operating temperature of 80° C. The matrix materials such as EPDM and SBR were mixed and blended for about 10 min initially and then nanoclay, nanosilica and curatives were added to it as per ASTM D15 [36]. The compounding formulations of the rubber composites with the filler materials are as stated in Table 1. The cross linking systems such are sulphur (S), dicumyl peroxide (DCP) and the mixed system consisting of sulphur and dicumyl peroxide (S + DCP) are indicated as S, P and M respectively. The nanocomposites containing sulphur system are labelled as $S_0$ (80/20/7.5/0 EPDM/SBR/NC/NS), $S_1$ (80/20/7.5/1 EPDM/SBR/NC/NS), and so on. Similarly, the nanocomposites containing dicumyl peroxide and mixed systems are labeled, as $P_0$ and $M_0$ respectively. The cure characteristics of the EPDM/SBR/NC/NS compounds were studied with the aid of an oscillating disc rheometer (ODR). The compounds are fabricated into thin sheets of 2 mmthickness via an electrically heated hydraulic press with a pressure of 30 MPa at a 160 °C for 10 min which was an optimum cure time.

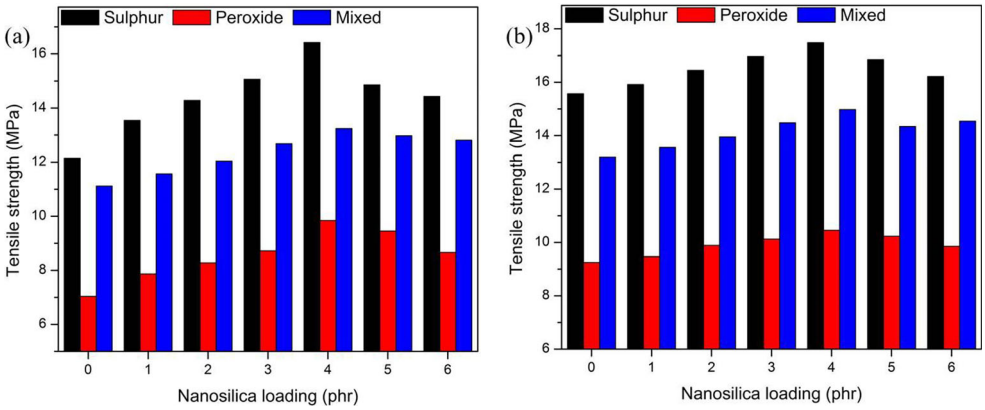


**Fig. 8** Tensile strength of EPDM/SBR-NC/NS composites: **a** Unaged, **b** Aged

## 2.4 Characterization

The rheological test of unvulcanized rubber samples was done as per ASTM D-2084 in an oscillating disc rheometer. The minimum torque, maximum torque, scorches time, optimum cure time and cure rate index (CRI) are measured. CRI was calculated using the equation.

$$CRI = \frac{100}{Optimum\ cure\ time - Scorch\ time} \tag{1}$$

The tensile test and tear test were performed as per ASTM standards D 412-C and D 624-B in the universal testing machine – series 7200 by Dak System Inc. (model: T-72102) with a crosshead speed of 500 mm/min. The hardness of the composite samples was measured in Shore-A Durometer as per ASTM D-2240. The tests were performed for both unaged and aged composite samples. For ageing, the sample was heated at 100 °C in an air circulating oven for 96 h and then cooled for 30 min at room temperature.

The crosslinking density of the sample was been calculated by using the following equation shown below in eq. (2) [37–39].

$$\vartheta\left(\frac{mol}{cm^3}\right) = \frac{1}{2M_c} \tag{2}$$

where, $M_c$ = Molar mass of the polymer between crosslink which is determined by the Flory-Rehner equation as stated below in eq. (3) [37–40].

$$M_c\left(\frac{g}{mol}\right) = \frac{-\rho_p V_s V_r^{1/3}}{\ln(1-V_r) + V_r + \chi V_r^2} \tag{3}$$

where, $\rho_p$ is the density of the polymer, $V_s$ is the molar volume of the solvent (106.3 mL/gmol), $V_r$ is the volume fraction of polymer in the solvent-swollen filled compound, $\chi$ is the interaction parameter of the polymer (0.3) [41], and $V_r$ is given by following eq. (4) [42].

$$V_r = \frac{1}{1+Q_m} \tag{4}$$

where, $Q_m$ is the weight swell of the EPDM/SBR nanocomposites in toluene.

The rebound resilience of the nanocomposites was carried out as per ASTM D-2632 standard. The abrasion resistance of the rubber nanocomposites in terms of volume loss was determined by DIN abrader (ZwickAbrasion tester, model 6102) according to ASTM D-5963. Abrasion loss was calculated using the eq. (5) as stated below:

$$Abrasion\ loss\ (mm^3) = \frac{\Delta m \times S_0}{\rho \times S} \tag{5}$$

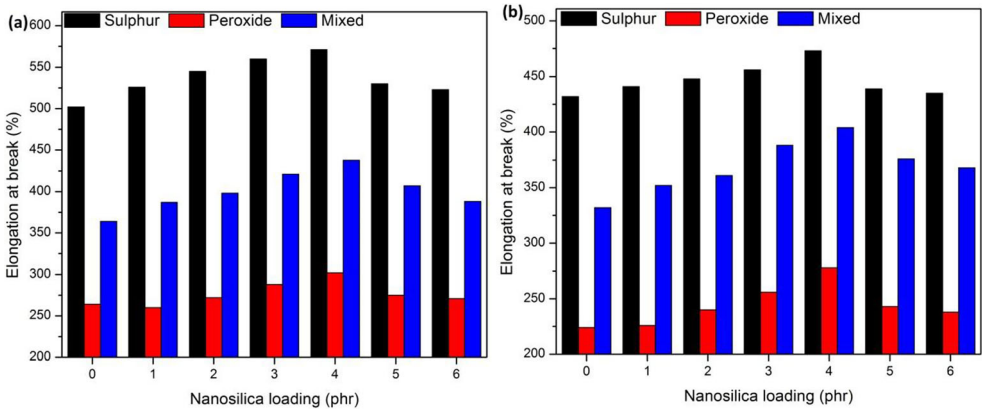


**Fig. 9** Elongation at break of EPDM/SBR-NC/NS composites: **a** Unaged, **b** Aged

where, Δm is a mass loss (mg); ρ is a density (mg/mm$^3$); $S_0$ is a value of nominal abrasive power (200 mg); S is an average abrasive power (mg).

The swelling test was done as per ASTM D-471 by the solvent immersion method. Swelling test was carried out at different penetrant such as aromatic (benzene, toluene, xylene and mesitylene), aliphatic (n-pentane, n-hexane, n-heptane and n-octane) and chlorinated hydrocarbons (dichloromethane, chloroform, and carbon tetrachloride). The mole percent uptake, $Q_t$ for solvent was determined using the formula.

$$Q_t(mol\%) = \frac{(M_t - M_0)/MW}{M_0} \times 100 \quad (6)$$

where, $M_0$ is the initial mass of the specimen, $M_t$ is the mass of the specimen after time 72 h of immersion, and MW is the molecular weight of the solvent.

Compression set test was carried out according to ASTMD-395. The compression set was determined using formula

$$Percentage\ of\ compression\ set, C\% = \frac{t_0 - t_1}{t_0 - t_s} \times 100 \quad (7)$$

where, $t_0$ is the original thickness of the specimen, $t_1$ is the specimen thickness after test and $t_s$ is the spacer bar thickness which is used.

Field emission-scanning electron microscopy (HitachiS-4160, Japan) was used to study the morphology of the fractured surface after coating it with a layer of gold particles.

## 3 Results and Discussions

### 3.1 Rheometric Characteristics

Minimum torque, maximum torque, torque difference (delta torque), scorch time, optimum cure time and cure rate index of EPDM/SBR composites reinforced with nanoclay and nanosilica and crosslinked with sulphur, peroxide and mixed system was shown in Figs. 2, 3, 4, 5, 6 and 7. The minimum torque has a direct relation with the viscosity of the compounds at the test temperature. The minimum torque can be calculated as the measure of the viscosity of the masticated rubber. From Fig. 2, the minimum torque increases with increase in the content of nanosilica for all three crosslinking systems. This indicates that the processability of the nanocomposites was adversely affected by the introduction of nanosilica in it. Peroxide and mixed system cured nanocomposites show a slight higher viscosity than that of sulphur cured nanocomposites. The higher viscosity of the nanocomposites may be due to the better interaction between nanosilica and the EPDM/SBR-NC compounds. The lower particle size of silica having a higher surface area, and hence, can have improved interactions.

The maximum torque value can be related to the measure of stock modulus [43]. The nanosilica loaded EPDM/SBR-NC composites show that maximum torque increases with increasing in the concentration of nanosilica for all crosslinking systems, as shown in Fig. 3. The delta torque is an indirect indicationof the degree of crosslinking of the rubber vulcanizates [44]. This shows that torque difference (delta torque) increase continuously with increase in the content of nanosilica for different curing system, as shown in Fig. 4. The results (Figs. 5 and 6) show that scorch time and optimum cure time of the rubber compositereduces with increase of nanosilica content in it. These results are in accordance with the previous work indicating a decrease in scorch protection of the nanocomposites with increasing nanosilica surface area [31]. Among the three different vulcanization systems, the scorch safety was highest for peroxide cured system followed sulphur cured ones. The Fig. 7 shows the cure rate index of the EPDM/SBR nanocomposites. Cure rate index for the EPDM/SBR nanocomposites was found to increase with increased nanosilica content for all vulcanizing systems. Therefore, nanosilica is the cure-activating material for the nanocomposites. A high cure rate index value shows higher vulcanization rate. The sulphur cured systems have been found to show the highest cure rate.

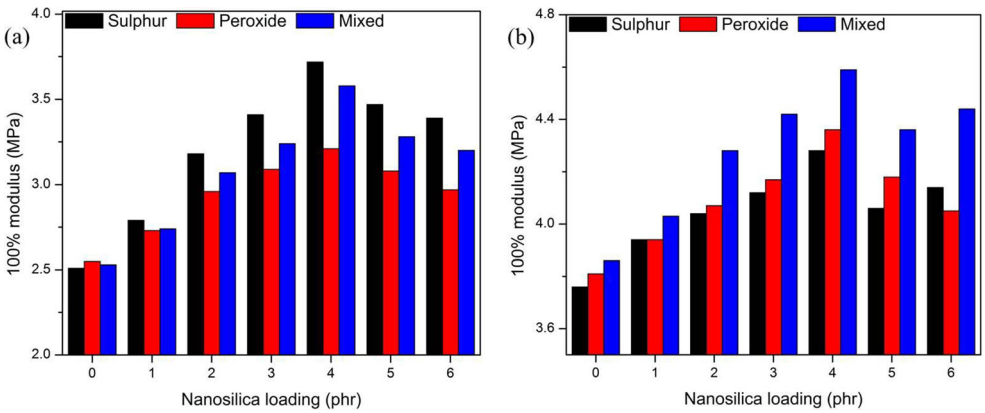


**Fig. 10** 100% modulus of EPDM/SBR-NC/NS composites: **a** Unaged, **b** Aged

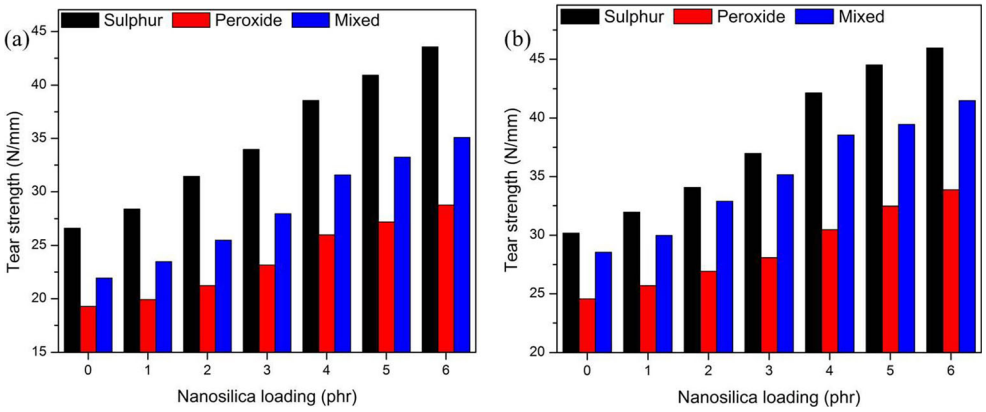


**Fig. 11** Tear strength of EPDM/SBR-NC/NS composites: **a** Unaged, **b** Aged

## 3.2 Mechanical Properties

The Fig. 8, shows the graph for the tensile strength of the EPDM/SBR nanocomposites reinforced with nanoclay and nanosilica. The tensile strength of the EPDM/SBR nanocomposites steps-up initially with increase in the concentration of nanosilica, and then decreases slowly with further increase in nanosilica concentration. From Fig. 9, it is also apparent that the optimal concentration of nanosilica was 4 phr after which the tensile strength drops down for all three curing systems. This was due to the better crosslink density observed at 4 phr of nanosilica as shown in Fig. 15. Figure 8 (a) clearly shows that the efficiency of nanosilica was improved with the presence of nanoclay. This was due to better interaction between the nanosilica and the EPDM/SBR matrix through nanoclay surface. And this was also owed to the adsorption of accelerator by silanol groups on the surface of silica. It was well known that the use of Si-69 would decrease the adsorption of accelerator on the surface of silica, the amount of Si-69 used in this work may be insufficient when the nanosilica content is high. It is known that nanosilica has strong filler-filler interaction. Thus, the increase in nanosilica content should lead to increases in the nanosilica-nanosilica interaction and, which leads to the decrease in nanosilica-EPDM/SBR/NC interaction. The thermally aged hybrid composites, shows a significant increase in the ultimate tensile strength (Fig. 8(b)). This was due to the development of more crosslinks formed during the thermal ageing process as shown in crosslink density values. Sulphur vulcanized system exhibit the highest tensile strength before and after thermal ageing compared to other two systems.

The Fig. 9 shows the increase in the elongation at break of the EPDM/SBR nanocomposites. The elongation at break of the EPDM/SBR nanocomposites increases initially and then decreases with increase in the concentration of nanosilica in it for all three curing systems. The elongation at break of the nanosilica filled hybrid rubber composites results from a compound relationship involving the properties of unlike constituent phases such as EPDM, SBR, nanoclay, nanosilica and their interfacial area. The nanosilica along with silane coupling agent increases the strong interaction between the EPDM/SBR-NC and nanosilica, which results in improvement in the properties of the hybrid composites. The ageing of hybrid composites shows a decrease in elongation at break when compared to ambient temperature due to oxidative degradation and chain scission. The increase in the crosslinking density after ageing decreases the mobility of the rubber chains. Sulphur vulcanized system shows the maximum elongation at break before and after thermal ageing compared to peroxide and mixed system.

Fig. 10 shows the modulus at 100% of the EPDM/SBR nanocomposites reinforced with nanoclay and nanosilica

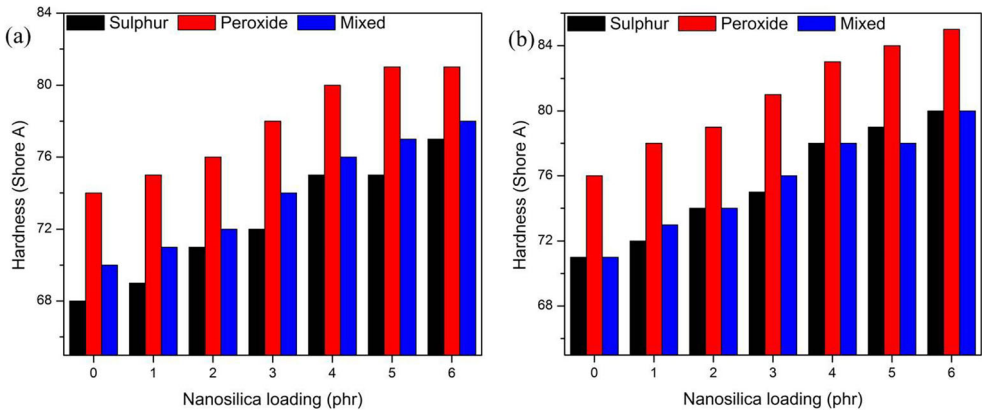


**Fig. 12** Hardness of EPDM/SBR-NC/NS composites: **a** Unaged, **b** Aged

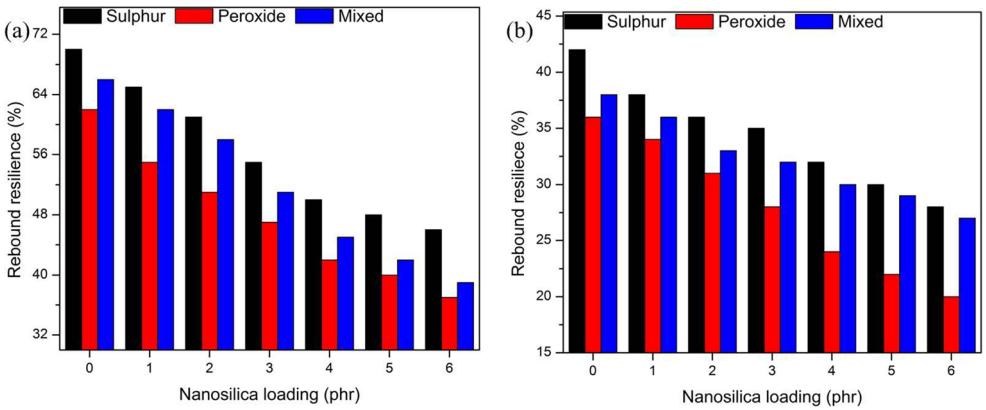


**Fig. 13** Rebound resilience of EPDM/SBR-NC/NS composites: **a** Unaged, **b** Aged

particles. With the incorporation of nanoparticles, the 100% modulus of the EPDM/SBR nanocomposites containing nanosilica steps-up with increase in the filler content upto 4 phr and then decreases gradually. This was due to the increase in crosslink density and the limitation of molecular chain mobility. The increase in modulus of aged composite over unaged one shows the increase of crosslink network as a result of post-curing during ageing treatment. Sulphur vulcanized composite exhibits a highest modulus before thermal ageing compared to peroxide and mixed system. After ageing, mixed system vulcanized composite exhibits the highest modulus compared to other systems.

The tear strength of the unaged and aged hybrid composites with various crosslinking systems was shown in Fig. 11. The tear strength of EPDM/SBR hybrid composites filled with nanoclay and nanosilica was increased with increase the in concentration of nanosilica. The improvement in tear strength was due to the increase in polymer chain rigidity, crosslink density and interaction among them. Sulphur vulcanized system exhibit a maximum tear strength before and after thermal ageing compared to the other two systems. All the types of thermally aged composites show a significant increase in the tear strength.

The hardness of EPDM/SBR hybrid composite reinforced with nanoclay and nanosilica increase with increase in the concentration of nanosilica as shown in Fig. 12. The increase in the hardness was due to the increase in interaction, crosslinking density and polymer chain rigidity in the polymer [13]. The two (nanoclay and nanosilica) nanoparticles in the composite penetrate through the void in matrix as well as interacted with matrix, which acts as physical crosslink that results in increasing of crosslink density [45, 46]. Higher crosslinking density leads to maximum hardness of the composite sample. The crosslink density makes the softer matrix

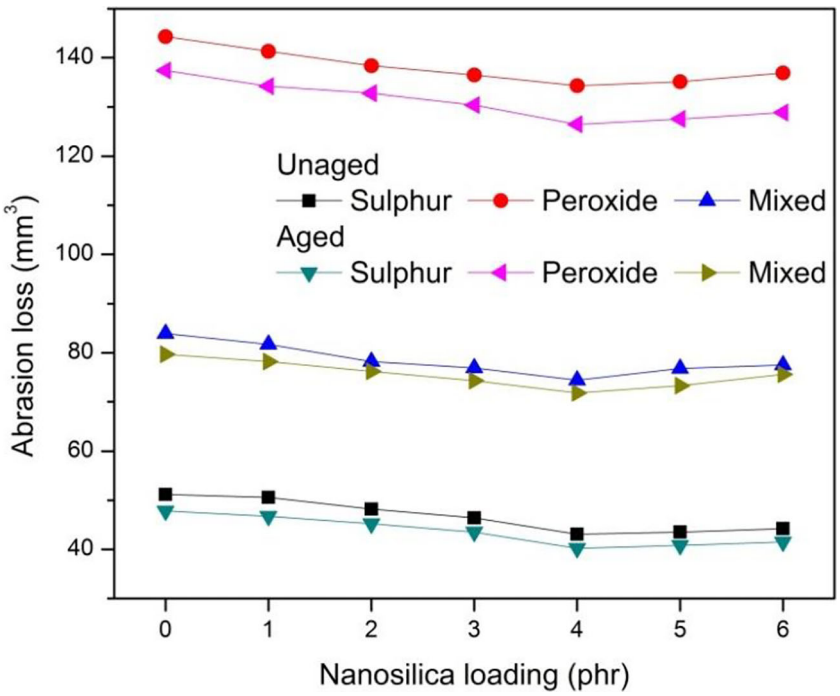


**Fig. 14** Abrasion loss of EPDM/SBR-NC/NS composites

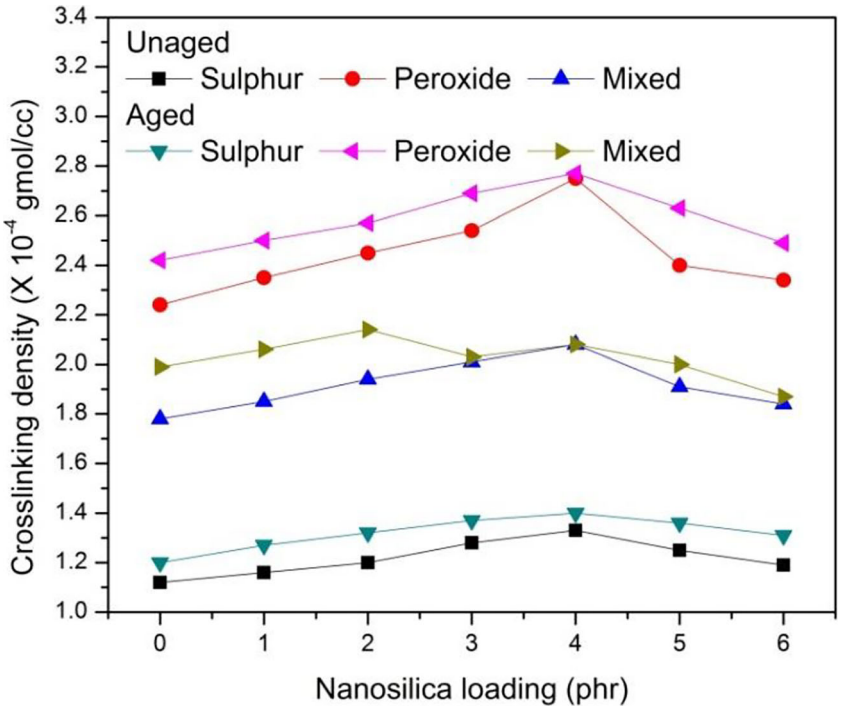


**Fig. 15** Crosslinking density of EPDM/SBR-NC/NS composites

into harder one. Peroxide cured system exhibits the highest hardness of unaged and aged nanocomposites compared to the other two systems.

The rebound resilience of the unaged and aged hybrid composites with different crosslinking systems are shown in Fig. 13. The hybrid composites that possess low rebound resilience have higher hardness. With the incorporation of nanosilica, the rebound resilience of the EPDM/SBR hybrid composites decreases with increase in its content. This was due to the restriction of mobility of polymer chain and due to increase in the crosslink density of the composite. The rebound resilience was minimal for the composite which was enriched in nanosilica, because nanosilica plays a vital role with the EPDM/SBR composite. The aged nanocomposites experiences

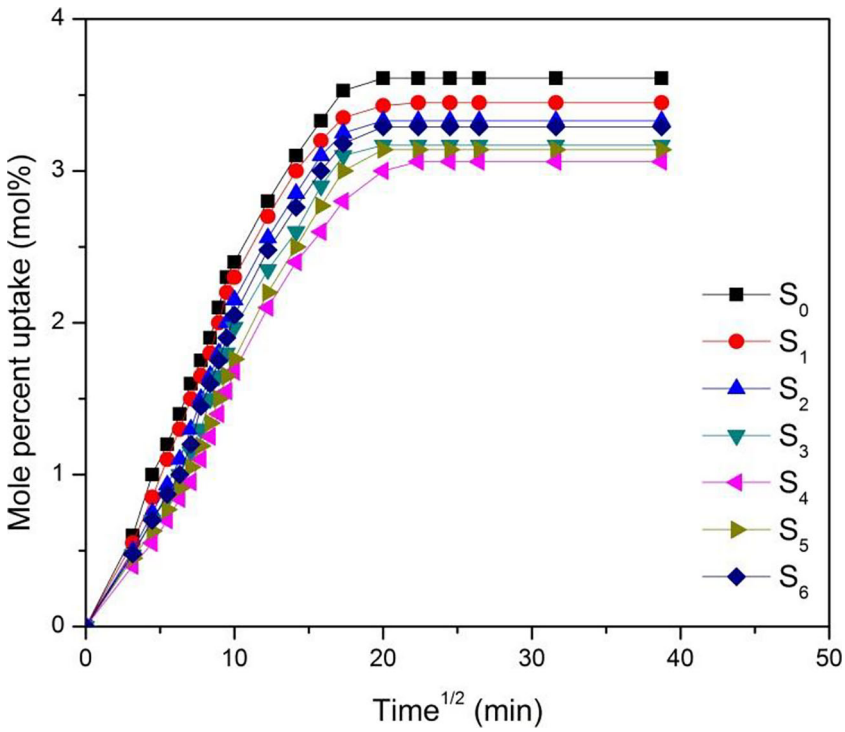


**Fig. 16** Mole percent intake vs Time for benzene

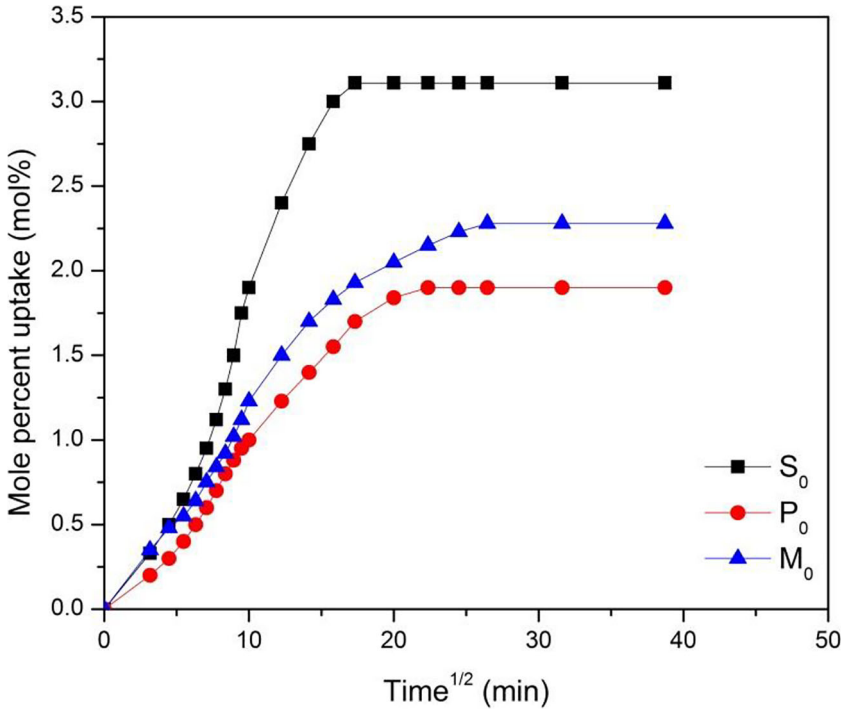


**Fig. 17** Mole percent uptake vs Time for toluene

lower rebound resilience than that of unaged composites at the same concentration of nanosilica. The reduction of rebound resilience of those rubber composites probably increases the crosslinking density of the material. The sulphur cured system exhibits the highest rebound resilience of unaged and aged nanocomposites compared to the other two systems.

Figure 14 shows the graph for the DIN abrasion test in terms of volume loss for the rubber hybrid composites. The wear resistance increase with increase in the concentration of nanosilica upto 4 phr and then starts to steps down for all the crosslinking systems used. This was due to the presence of nanosilica, which can hinder the deformation of the composite during abrasion process. The combination of nanoclay and

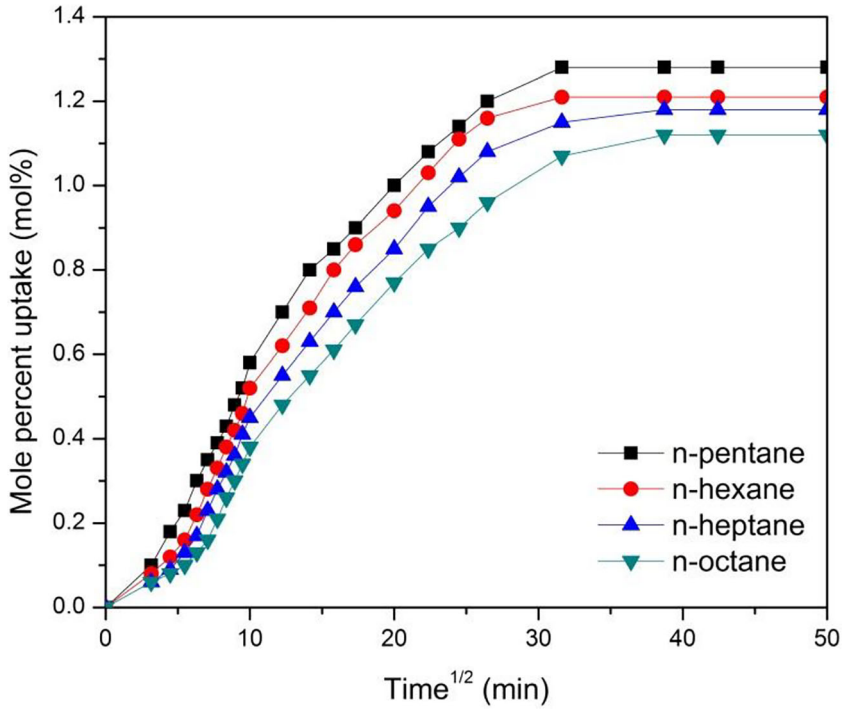


**Fig. 18** Mole percent uptake vs Time for peroxide

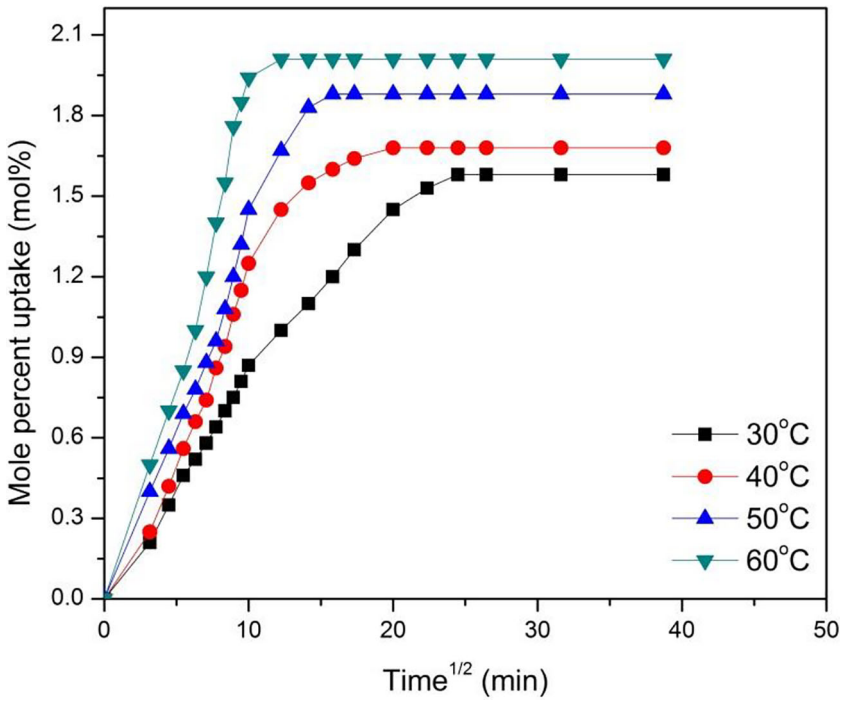


**Fig. 19** Temperature dependence of the mixed system crossliked 4 phrnanosilica filled nanocomposites in carbon tetrachloride

**Table 2** Mole percent uptake of aromatic, aliphatic and chlorinated penetrant of EPDM/SBR-NC/NS composites at 30 °C

| Sample code | Mole percent uptake (mol%) at 30 °C | | | | | | | | | | |
|---|---|---|---|---|---|---|---|---|---|---|---|
| | Aromatic | | | | Aliphatic | | | | Chlorinated | | |
| | Benzene | Toluene | Xylene | Mesitylene | n-pentane | n-hexane | n-heptane | n-octane | Dichloromethane | Chloroform | Carbon tetrachloride |
| $S_0$ | 3.61 | 3.11 | 2.47 | 2.22 | 1.97 | 1.92 | 1.87 | 1.82 | 4.45 | 4.02 | 1.88 |
| $S_1$ | 3.45 | 3.03 | 2.35 | 2.14 | 1.9 | 1.86 | 1.79 | 1.73 | 4.18 | 3.75 | 1.8 |
| $S_2$ | 3.33 | 2.95 | 2.27 | 2.08 | 1.84 | 1.8 | 1.72 | 1.65 | 4 | 3.59 | 1.73 |
| $S_3$ | 3.17 | 2.83 | 2.2 | 2.02 | 1.78 | 1.72 | 1.66 | 1.6 | 3.89 | 3.45 | 1.68 |
| $S_4$ | 3.06 | 2.75 | 2.14 | 1.95 | 1.73 | 1.7 | 1.62 | 1.54 | 3.8 | 3.3 | 1.64 |
| $S_5$ | 3.14 | 2.86 | 2.25 | 1.98 | 1.78 | 1.74 | 1.68 | 1.6 | 3.88 | 3.42 | 1.66 |
| $S_6$ | 3.29 | 2.94 | 2.32 | 2.11 | 1.89 | 1.82 | 1.75 | 1.69 | 3.97 | 3.55 | 1.75 |
| $P_0$ | 2.29 | 2.01 | 1.84 | 1.85 | 1.58 | 1.54 | 1.48 | 1.45 | 2.95 | 2.77 | 1.7 |
| $P_1$ | 2.2 | 1.94 | 1.75 | 1.75 | 1.45 | 1.42 | 1.37 | 1.33 | 2.8 | 2.52 | 1.6 |
| $P_2$ | 2.15 | 1.88 | 1.72 | 1.71 | 1.38 | 1.34 | 1.3 | 1.25 | 2.72 | 2.41 | 1.53 |
| $P_3$ | 2.08 | 1.83 | 1.68 | 1.66 | 1.31 | 1.28 | 1.25 | 1.17 | 2.66 | 2.34 | 1.47 |
| $P_4$ | 2.02 | 1.73 | 1.6 | 1.57 | 1.28 | 1.21 | 1.18 | 1.12 | 2.6 | 2.28 | 1.44 |
| $P_5$ | 2.15 | 1.89 | 1.73 | 1.72 | 1.35 | 1.26 | 1.24 | 1.19 | 2.68 | 2.36 | 1.49 |
| $P_6$ | 2.19 | 1.92 | 1.79 | 1.76 | 1.39 | 1.32 | 1.29 | 1.22 | 2.76 | 2.42 | 1.55 |
| $M_0$ | 2.58 | 2.28 | 2.06 | 2 | 1.97 | 1.9 | 1.86 | 1.8 | 3.47 | 3.02 | 1.81 |
| $M_1$ | 2.45 | 2.21 | 1.98 | 1.96 | 1.9 | 1.82 | 1.79 | 1.68 | 3.33 | 2.87 | 1.72 |
| $M_2$ | 2.38 | 2.14 | 1.92 | 1.92 | 1.85 | 1.75 | 1.7 | 1.6 | 3.23 | 2.77 | 1.66 |
| $M_3$ | 2.32 | 2.08 | 1.85 | 1.87 | 1.8 | 1.69 | 1.64 | 1.55 | 3.17 | 2.7 | 1.61 |
| $M_4$ | 2.15 | 2.03 | 1.8 | 1.8 | 1.76 | 1.64 | 1.58 | 1.51 | 3.13 | 2.63 | 1.58 |
| $M_5$ | 2.28 | 2.14 | 1.91 | 1.86 | 1.81 | 1.69 | 1.68 | 1.57 | 3.21 | 2.72 | 1.64 |
| $M_6$ | 2.36 | 2.19 | 1.96 | 1.91 | 1.86 | 1.76 | 1.74 | 1.63 | 3.26 | 2.78 | 1.68 |

**Table 3** Mole percent uptake of aromatic penetrant of EPDM/SBR-NC/NS composites at 40 °C, 50 °C, and 60 °C

| Sample code | Mole percent uptake (mol%) | | | | | | | | | | | |
|---|---|---|---|---|---|---|---|---|---|---|---|---|
| | Benzene | | | Toluene | | | Xylene | | | Mesitylene | | |
| | 40 °C | 50 °C | 60 °C | 40 °C | 50 °C | 60 °C | 40 °C | 50 °C | 60 °C | 40 °C | 50 °C | 60 °C |
| $S_0$ | 3.78 | 3.88 | 3.99 | 3.36 | 3.46 | 3.55 | 2.75 | 3.41 | 3.49 | 2.79 | 2.98 | 3.21 |
| $S_1$ | 3.6 | 3.8 | 3.93 | 3.25 | 3.38 | 3.48 | 2.64 | 3.2 | 3.35 | 2.7 | 2.92 | 3.15 |
| $S_2$ | 3.49 | 3.72 | 3.88 | 3.18 | 3.34 | 3.42 | 2.58 | 3.02 | 3.27 | 2.64 | 2.87 | 3.08 |
| $S_3$ | 3.35 | 3.66 | 3.84 | 3.11 | 3.26 | 3.36 | 2.5 | 2.92 | 3.21 | 2.57 | 2.82 | 3 |
| $S_4$ | 3.2 | 3.61 | 3.79 | 3.06 | 3.21 | 3.32 | 2.44 | 2.84 | 3.12 | 2.52 | 2.77 | 2.89 |
| $S_5$ | 3.32 | 3.65 | 3.85 | 3.13 | 3.25 | 3.35 | 2.52 | 2.9 | 3.15 | 2.58 | 2.83 | 2.95 |
| $S_6$ | 3.47 | 3.7 | 3.89 | 3.19 | 3.29 | 3.39 | 2.6 | 2.99 | 3.19 | 2.66 | 2.85 | 3.03 |
| $P_0$ | 2.44 | 2.54 | 2.63 | 2.13 | 2.23 | 2.35 | 1.96 | 2.09 | 2.22 | 1.93 | 2 | 2.1 |
| $P_1$ | 2.38 | 2.48 | 2.6 | 2.06 | 2.17 | 2.3 | 1.88 | 2.02 | 2.15 | 1.85 | 1.94 | 2.03 |
| $P_2$ | 2.32 | 2.42 | 2.54 | 2 | 2.14 | 2.25 | 1.82 | 1.97 | 2.1 | 1.8 | 1.88 | 1.96 |
| $P_3$ | 2.26 | 2.35 | 2.5 | 1.94 | 2.09 | 2.19 | 1.74 | 1.94 | 2.04 | 1.74 | 1.85 | 1.9 |
| $P_4$ | 2.24 | 2.3 | 2.46 | 1.88 | 2.04 | 2.15 | 1.68 | 1.9 | 2 | 1.67 | 1.8 | 1.85 |
| $P_5$ | 2.29 | 2.36 | 2.49 | 1.95 | 2.1 | 2.2 | 1.76 | 1.95 | 2.08 | 1.75 | 1.84 | 1.89 |
| $P_6$ | 2.36 | 2.41 | 2.54 | 2.03 | 2.16 | 2.24 | 1.85 | 1.99 | 2.1 | 1.88 | 1.89 | 1.96 |
| $M_0$ | 2.88 | 2.97 | 3.09 | 2.39 | 2.6 | 2.66 | 2.25 | 2.5 | 2.7 | 2.24 | 2.33 | 2.51 |
| $M_1$ | 2.77 | 2.91 | 3.03 | 2.31 | 2.5 | 2.61 | 2.12 | 2.42 | 2.6 | 2.13 | 2.27 | 2.44 |
| $M_2$ | 2.72 | 2.86 | 2.97 | 2.25 | 2.44 | 2.57 | 2.07 | 2.36 | 2.55 | 2.07 | 2.22 | 2.38 |
| $M_3$ | 2.67 | 2.82 | 2.92 | 2.2 | 2.39 | 2.53 | 2.01 | 2.3 | 2.49 | 1.99 | 2.18 | 2.33 |
| $M_4$ | 2.62 | 2.77 | 2.87 | 2.17 | 2.3 | 2.5 | 1.95 | 2.24 | 2.44 | 1.92 | 2.12 | 2.28 |
| $M_5$ | 2.69 | 2.84 | 2.93 | 2.26 | 2.36 | 2.54 | 2.03 | 2.29 | 2.5 | 1.97 | 2.19 | 2.35 |
| $M_6$ | 2.76 | 2.88 | 3.02 | 2.33 | 2.42 | 2.58 | 2.09 | 2.35 | 2.54 | 2.04 | 2.24 | 2.41 |

nanosilica will strongly affects the abrasion property of EPDM/SBR-NC/NS composites. The enhancement in the wear property was due to the homogeneous distribution of the dual reinforcement in the EPDM/SBR matrix that leads to a good matrix – reinforcement interaction. At 4 phr nanosilica content, an EPDM/SBR-NC/NS hybrid composite exhibits a minimal wear loss than other composites, which was in accordance with its tensile property and hardness of the material. The sulphur cured system exhibit a higher wear resistance for both unaged and aged hybrid composites compared to others. The wear resistance of EPDM/SBR hybrid composites relay on its modulus, strength, resilience, frictional behavior (friction coefficient) and fatigability [13, 47, 48] of the composite sample. The maximal wear resistance of the hybrid composite could be due to the synergistic effect of different nanoparticles present in the system. Higher crosslink density of the composite was responsible for higher abrasion resistance. As the crosslink density increases, the softer rubber matrix turns into harder one. The abrasion loss of thermally aged samples decreases as compared to the corresponding unaged samples due to the increase in the crosslink density of the composite. The composite with uniform distribution of nanoparticles was apparent to have a better wear resistance than that of with aggloramated ones (Fig. 15).

### 3.3 Swelling Properties

The effect of nanosilica content on the swelling properties of penetrant (benzene, toluene, xylene, mesitylene, n-pentane, n-hexane, etc.,) through EPDM/SBR-NC/NS hybrid composites was investigated. The swelling behavior of the hybrid composites was dependent on the type of rubber matrix, reinforcing material, temperature, penetrant, curing agent, etc., used. The Figs. 16, 17, 18 and 19 and Tables 2, 3, 4 and 5 shows the swelling properties of the hybrid composites reinforced with nanoclay and nanosilica. The effects of nanosilica loading, vulcanizing agents, nature of penetrants and the temperature on mole percent uptake in the hybrid composites were analyzed. The swelling curves plotted are for the mole percent uptake ($Q_t$) and the square root of time ($t^{1/2}$).

The Fig. 16 indicates the mole percent uptake of benzene penetrant with different content of nanosilica vulcanized with sulphur at 30 °C. The mole percent uptake decreases initially, attains an optimum value, and then increases with increasing the nanosilica content. From the Fig. 16, it was clear that, the

**Table 4** Mole percent uptake of aliphatic penetrant of EPDM/SBR-NC/NS composites at 40 °C, 50 °C, and 60 °C

| Sample code | Mole percent uptake (mol%) | | | | | | | | | | | |
|---|---|---|---|---|---|---|---|---|---|---|---|---|
| | n-pentane | | | n-hexane | | | n-heptane | | | n-octane | | |
| | 40 °C | 50 °C | 60 °C | 40 °C | 50 °C | 60 °C | 40 °C | 50 °C | 60 °C | 40 °C | 50 °C | 60 °C |
| $S_0$ | 2.08 | 2.33 | 2.46 | 2.17 | 2.25 | 2.41 | 2.02 | 2.15 | 2.31 | 2.04 | 2.12 | 2.28 |
| $S_1$ | 2.02 | 2.28 | 2.4 | 2.08 | 2.17 | 2.35 | 1.94 | 2.08 | 2.25 | 1.92 | 2.04 | 2.21 |
| $S_2$ | 1.96 | 2.22 | 2.35 | 2.02 | 2.12 | 2.28 | 1.88 | 2.02 | 2.18 | 1.84 | 1.96 | 2.16 |
| $S_3$ | 1.9 | 2.17 | 2.29 | 1.95 | 2.07 | 2.21 | 1.83 | 1.97 | 2.14 | 1.78 | 1.91 | 2.11 |
| $S_4$ | 1.84 | 2.12 | 2.25 | 1.9 | 2.03 | 2.17 | 1.77 | 1.91 | 2.06 | 1.71 | 1.84 | 2.07 |
| $S_5$ | 1.92 | 2.18 | 2.3 | 1.97 | 2.08 | 2.24 | 1.82 | 1.96 | 2.09 | 1.8 | 1.88 | 2.12 |
| $S_6$ | 1.98 | 2.23 | 2.36 | 2 | 2.11 | 2.29 | 1.86 | 2 | 2.13 | 1.85 | 1.92 | 2.17 |
| $P_0$ | 1.87 | 2 | 2.1 | 1.85 | 1.96 | 2.04 | 1.83 | 1.9 | 2 | 1.57 | 1.66 | 1.91 |
| $P_1$ | 1.78 | 1.92 | 2.04 | 1.77 | 1.91 | 1.99 | 1.76 | 1.83 | 1.94 | 1.5 | 1.6 | 1.85 |
| $P_2$ | 1.73 | 1.87 | 1.98 | 1.7 | 1.88 | 1.95 | 1.72 | 1.77 | 1.9 | 1.45 | 1.54 | 1.78 |
| $P_3$ | 1.67 | 1.82 | 1.93 | 1.65 | 1.82 | 1.92 | 1.61 | 1.72 | 1.85 | 1.39 | 1.5 | 1.75 |
| $P_4$ | 1.63 | 1.78 | 1.87 | 1.61 | 1.77 | 1.87 | 1.55 | 1.68 | 1.81 | 1.35 | 1.45 | 1.67 |
| $P_5$ | 1.69 | 1.81 | 1.94 | 1.69 | 1.8 | 1.93 | 1.62 | 1.74 | 1.85 | 1.41 | 1.48 | 1.72 |
| $P_6$ | 1.75 | 1.86 | 1.98 | 1.74 | 1.83 | 1.98 | 1.68 | 1.79 | 1.89 | 1.46 | 1.53 | 1.78 |
| $M_0$ | 2.21 | 2.28 | 2.39 | 2.03 | 2.16 | 2.21 | 1.95 | 2.04 | 2.15 | 1.94 | 2.1 | 2.14 |
| $M_1$ | 2.16 | 2.2 | 2.32 | 1.98 | 2.09 | 2.15 | 1.89 | 1.98 | 2.09 | 1.9 | 2.01 | 2.06 |
| $M_2$ | 2.08 | 2.14 | 2.25 | 1.91 | 2.05 | 2.11 | 1.82 | 1.91 | 2.04 | 1.82 | 1.9 | 2.01 |
| $M_3$ | 2.01 | 2.08 | 2.17 | 1.87 | 2 | 2.08 | 1.77 | 1.88 | 2 | 1.75 | 1.86 | 1.95 |
| $M_4$ | 1.97 | 2.05 | 2.12 | 1.82 | 1.94 | 2.02 | 1.72 | 1.82 | 1.94 | 1.69 | 1.79 | 1.92 |
| $M_5$ | 2.03 | 2.12 | 2.21 | 1.88 | 1.98 | 2.12 | 1.78 | 1.89 | 1.99 | 1.74 | 1.86 | 1.97 |
| $M_6$ | 2.09 | 2.19 | 2.27 | 1.94 | 2.06 | 2.18 | 1.85 | 1.94 | 2.04 | 1.79 | 1.91 | 2.03 |

optimum nanosilica content was 4 phr, and a further incorporation of the nanoparticles in it will increase the mole percent uptake to a considerable extent. The mole percent uptake versus square root of time curve shows two different sections; an initial steep section with high swelling rate due to large concentration gradient and the final section with a reduced swelling rate that ultimately reaches swelling equilibrium. The equilibrium benzene uptake of EPDM/SBR hybrid composites reduced with increase in the concentration nanosilica in it. Beyond 4 phr the benzene uptake increases a little due to the formation of nanosilica agglomerates. The improvement in swelling resistance was due to the good interaction between the fillers (nanosilica/nanoclay) and rubber matrix. The trend similar to this was observed for aromatic (toluene, xylene and mesitylene), aliphatic (n-pentane, n-hexane, n-heptane and n-octane) and chlorinated (dichloromethane, chloroform and carbon tetrachloride) hydrocarbons and are clearly stated in Table 2. The decline of swelling resistance at higher concentration of nanosilica was due to the increase in nanosilica-nanosilica interaction which results in weakening interaction between the reinforcement and the rubber matrix.

The Fig. 17 clearly shows that the peroxide vulcanized composite absorbs a lesser amount of solvent whereas the sulphur vulcanized composites absorbs a greater amount. The swelling resistance of the rubber hybrid composites was normally related to their crosslink degree and polymer-solvent interactions. In this study the composites with the similar composition and crosslinked with peroxide exhibits a lower values in mole percent uptake than to those system crosslinked with the sulphur. This may be due to the higher crosslink degree and structure of crosslinks observed in sulphur system. The trend similar to this was observed with aromatic, aliphatic and chlorinated hydrocarbons as stated in Table 2. The effect of penetrant size on the mole percent uptake of aliphatic hydrocarbons (n-pentane, n-hexane, n-heptane and n-octane) of 4 phr nanosilica composites vulcanized with peroxide was shown in Fig. 12. The penetrant size was found to be maximum for n-octane followed by n-heptane, n-hexane and n-pentane. The higher molecular weight of the penetrant exhibits a lowest uptake and vice versa. In general, the molecular weight and penetrant are inversely proportional to them. From the Fig. 18, it was clear that the trend was in the order n-pentane > n-hexane >n-heptane > n-octane. A trend similar to this was observed with aromatic, aliphatic and chlorinated hydrocarbons and was tabulated in Table 2. The higher molecular weight (153.82 g/mol) of the carbon tetrachloride

**Table 5** Mole percent uptake of chlorinated penetrant at 40 °C, 50 °C, and 60 °C, and compression set of EPDM/SBR-NC/NS composites

| Sample code | Mole percent uptake (mol%) | | | | | | | | | Compression set (%) | | | | |
|---|---|---|---|---|---|---|---|---|---|---|---|---|---|---|
| | Dichloromethane | | | Chloroform | | | Carbon tetrachloride | | | For 1 day at 23 °C | For 2 days at 23 °C | For 3 days at 23 °C | For 1 day at 70 °C | For 1 day at 100 °C |
| | 40 °C | 50 °C | 60 °C | 40 °C | 50 °C | 60 °C | 40 °C | 50 °C | 60 °C | | | | | |
| $S_0$ | 4.67 | 4.85 | 5 | 4.28 | 4.45 | 4.68 | 2 | 2.08 | 2.23 | 6.72 | 11.52 | 17.97 | 23.76 | 28.05 |
| $S_1$ | 4.6 | 4.78 | 4.91 | 4.22 | 4.38 | 4.63 | 1.93 | 2.02 | 2.17 | 7.25 | 13.13 | 19.12 | 25.45 | 30.42 |
| $S_2$ | 4.51 | 4.72 | 4.86 | 4.17 | 4.35 | 4.55 | 1.88 | 1.97 | 2.12 | 7.98 | 14.87 | 20.56 | 28.18 | 33.25 |
| $S_3$ | 4.45 | 4.65 | 4.81 | 4.08 | 4.3 | 4.49 | 1.83 | 1.91 | 2.08 | 8.56 | 16.05 | 21.98 | 30.41 | 35.64 |
| $S_4$ | 4.38 | 4.6 | 4.75 | 4 | 4.26 | 4.43 | 1.77 | 1.85 | 2.03 | 9.62 | 17.74 | 23.15 | 32.58 | 37.15 |
| $S_5$ | 4.46 | 4.67 | 4.82 | 4.09 | 4.26 | 4.51 | 1.8 | 1.89 | 2.09 | 10.75 | 18.56 | 24.56 | 34.56 | 40.08 |
| $S_6$ | 4.52 | 4.74 | 4.88 | 4.16 | 4.29 | 4.58 | 1.87 | 1.96 | 2.15 | 12.16 | 19.79 | 25.16 | 36.74 | 43.15 |
| $P_0$ | 3.08 | 3.21 | 3.47 | 2.98 | 3.14 | 3.32 | 1.84 | 2.02 | 2.16 | 3.27 | 5.88 | 9.07 | 10.32 | 10.46 |
| $P_1$ | 3.02 | 3.14 | 3.4 | 2.92 | 3.08 | 3.27 | 1.78 | 1.94 | 2.04 | 3.56 | 6.33 | 9.87 | 11.58 | 12.08 |
| $P_2$ | 2.92 | 3.08 | 3.34 | 2.84 | 3.03 | 3.22 | 1.73 | 1.88 | 2.01 | 3.97 | 6.85 | 10.56 | 12.75 | 13.76 |
| $P_3$ | 2.87 | 3 | 3.3 | 2.76 | 2.98 | 3.17 | 1.68 | 1.83 | 1.95 | 4.54 | 7.47 | 11.15 | 14.25 | 15.25 |
| $P_4$ | 2.85 | 2.95 | 3.24 | 2.7 | 2.91 | 3.11 | 1.63 | 1.78 | 1.9 | 5.03 | 8.04 | 11.87 | 15.89 | 16.96 |
| $P_5$ | 2.94 | 3.02 | 3.28 | 2.75 | 2.98 | 3.14 | 1.66 | 1.86 | 1.96 | 5.56 | 8.86 | 12.68 | 17.33 | 18.14 |
| $P_6$ | 2.98 | 3.09 | 3.34 | 2.81 | 3.04 | 3.19 | 1.73 | 1.9 | 1.99 | 6.13 | 9.54 | 14.27 | 18.68 | 20.26 |
| $M_0$ | 3.6 | 3.75 | 3.95 | 3.21 | 3.45 | 3.66 | 1.91 | 2.05 | 2.2 | 4.86 | 8.74 | 13.23 | 14.94 | 17.07 |
| $M_1$ | 3.5 | 3.68 | 3.88 | 3.14 | 3.38 | 3.59 | 1.85 | 2.01 | 2.14 | 5.26 | 9.56 | 14.28 | 17.14 | 19.26 |
| $M_2$ | 3.42 | 3.6 | 3.81 | 3.05 | 3.32 | 3.52 | 1.77 | 1.98 | 2.1 | 5.89 | 10.15 | 15.16 | 18.87 | 21.23 |
| $M_3$ | 3.37 | 3.52 | 3.75 | 2.96 | 3.27 | 3.45 | 1.72 | 1.92 | 2.05 | 6.57 | 10.72 | 15.92 | 20.75 | 22.87 |
| $M_4$ | 3.32 | 3.46 | 3.71 | 2.9 | 3.22 | 3.41 | 1.68 | 1.88 | 2.01 | 7.04 | 11.52 | 16.67 | 22.23 | 24.25 |
| $M_5$ | 3.38 | 3.5 | 3.76 | 2.95 | 3.25 | 3.47 | 1.73 | 1.93 | 2.07 | 7.84 | 12.06 | 17.26 | 23.93 | 26.07 |
| $M_6$ | 3.44 | 3.56 | 3.83 | 3.03 | 3.31 | 3.53 | 1.77 | 1.97 | 2.13 | 8.48 | 12.76 | 18.05 | 25.26 | 27.64 |

exhibits a lowest uptake as compared to the other chlorinated hydrocarbons (84.93 g/mol for dichloromethane and 119.38 g/mol for chloroform).

The effect of temperature on the mole percent uptake of carbon tetrachloride in 4 phr nanosilica filled composites, vulcanized with mixed systems was shown in Fig. 19. The addition of nanosilica in the composite reduces the free spaces in the matrix and restricts the movement of the polymeric chain in the rubber composite. However, with an increase in the nanosilica content of more than 4 phr, there was a decrease in swelling resistance on the hybrid rubber composite. A similar trend was observed for swelling properties conducted at 40 °C, 50 °C and 60 °C also. As the temperature increases, the mole percent uptake also increases for all the hybrid composites [31]. As a result, the swelling resistance of the EPDM/SBR-NC/NS hybrid composites decreases at higher temperature. The mole percent uptake at 40 °C, 50 °C and, 60 °C are broadly tabulated in Tables 3, 4 and 5 respectively.

### 3.4 Compression Set

The compression set values of the EPDM/SBR hybrid composites was tabulated in Table 5. The hybrid composite without the presence of nanosilica shows a lower value in compression set. The compression set values of the hybrid composites increases with increase in the concentration of nanosilica. This may be due to the increase in the crosslinking density of the composite and decrease in the mobility of long polymeric chains, which result in the increase in the stiffness of the nanocomposites. The certain amount (25% strain) of compression (load) was applied to the rubber materials, the vast crosslinks attempt to the resistance of this load which stated as increasing the stiffness of the rubber samples. During this compression resistance some of the crosslinks have been broken; subsequently when the compression relieved the number of crosslinks responsible for this strain recovery was less than the number of crosslinks responsible to resist it. Henceforth, the samples were not recovered to its original thickness. As anticipated for increasing crosslinking density, the alteration to break more crosslinks increases which consequences in high percentage of compression set. This result was in accordance with Vishvanathperumal et al., [49]. The peroxide vulcanized system exhibits lower compression set and the sulphur vulcanized system show higher compression set. A similar trend was followed in compression set test at 23 °C, 70 °C and 100 °C. As the time and temperature

increases with the presence of nanosilica, the compression set values also gets increased. The compression set values of the material was to be lower inorder to make it better for use.

### 3.5 Morphology

The FESEM images of the tensile fractured specimen for the different composites are shown in Fig. 20(a-i). The FESEM micrograph having the composition of 7.5 phr of nanoclay and 1phr of nanosilica indicates a good dispersion of nanoclay and nanosilica in the EPDM/SBR matrix and are clearly shown in the Fig. 20 (a-c). The tensile-fractured surface of nanocomposite with 1 phr nanosilica exhibits a noticeably smoother plane than that of nanocomposite with 6 phr nanosilica. These Figures show a homogeneous phase with a fewer tear lines in it. Most of nanosilica was well enfolded in the rubber matrix, as shown in Fig. 20(a-c). From the above observations it was clear that that nanosilica had good dispersion in the matrix at lower loading conditions. The FESEM micrograph having the composition of 7.5 phr of nanoclay and 4 phr of nanosilica exhibits good dispersion of both fillers in the rubber matrix and are clearly shown in Fig. 20(d-f). The nanocomposite with low nanosilica content (4phr) displays a smooth surface and better nanosilica dispersion (Fig. 20d-f) than that with a high nanosilica concentration. $S_4$ shows the better dispersion and distribution of nanosilica particles in the EPDM/SBR matrix and hence better tensile strength was observed for the composite. The micrograph of S6, P6 and M6 reflects a poor dispersion of silica nanoparticles in the EPDM/SBR matrix as shown in Fig. 20(g-i). Agglomeration of nanosilica particles was observed in Fig. 20(h) which was due to strong interaction of silica-silica compounds.

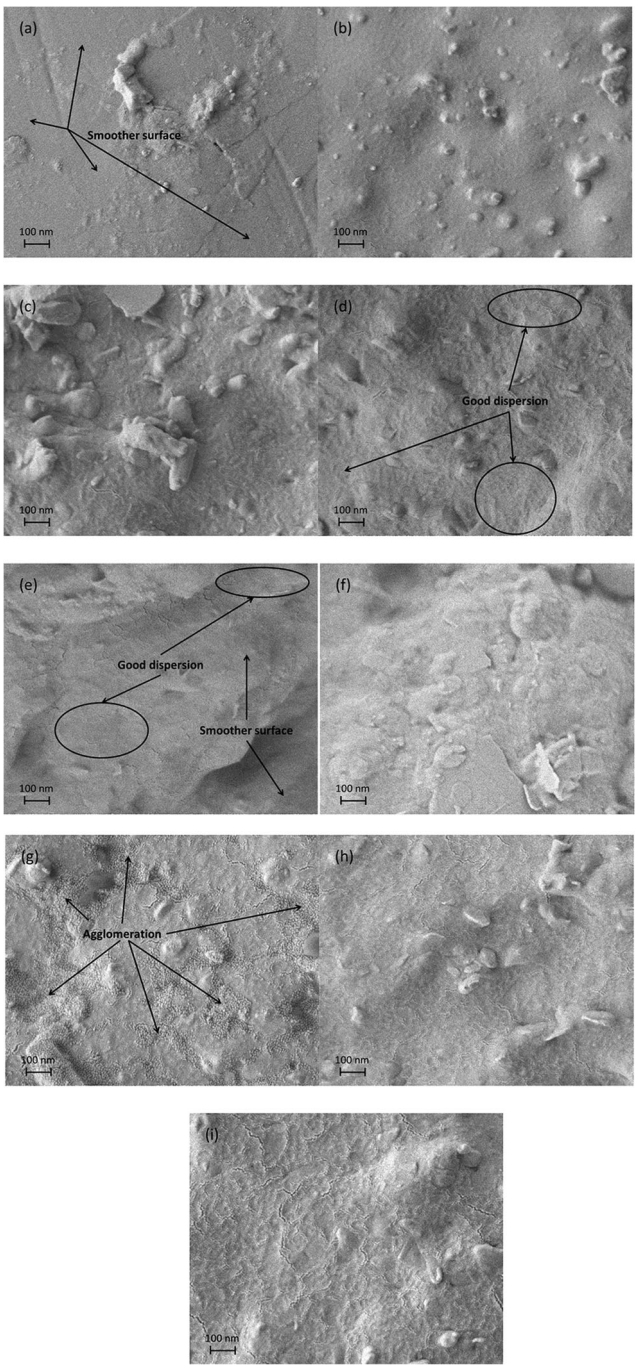


**Fig. 20** Tensile fracturedsurfaces with magnification 100 nm for different composites: **a** $S_1$, **b** $P_1$, **c** $M_1$, **d** $S_4$, **e** $P_4$, **f** $M_4$, **g** $S_6$, **h** $P_6$ and **i** $M_6$

## 4 Conclusions

A newer EPDM/SBR hybrid composite reinforced with nanoclay and nanosilica was successfully prepared. The synergistic effect of nanoclay and nanosilica in EPDM/SBR nanocomposites was investigated. The incorporation of nanosilica accelerates the vulcanizing reaction of EPDM/SBR composite compared to EPDM/SBR-NC composite. The prepared hybrid composite with NC and NS shows an improvement in tensile strength, elongation at break, modulus, tear strength, hardness, abrasion resistance and swelling resistance. The optimum filler content to obtain the best tensile properties was 4 phr. Hardness, tear strength and compression set of the composite increases with increase in the concentration of fillers in it whereas the rebound resilience of the composites have a negative impact in it. Among different vulcanizing systems, sulphur vulcanized hybrid composites exhibits the best mechanical properties (tensile strength, elongation at break, modulus and tear strength) rebound resilience and abrasion resistance, whereas the peroxide vulcanized nanocomposites shows the better hardness, swelling resistance and compression set. Due to thermal ageing (at 100 °C) the tensile strength, 100% modulus, hardness, tear strength and abrasion resistance increase whereas the elongation at break and rebound resilience of the hybrid EPDM/SBR nanocomposites decrease. The tensile strength, elongation at break, tear strength and hardness for sulphur cured EPDM/SBR nanocomposites filled with NC/NS increases to

35%, 14%, 64% and 13% respectively as compared to EPDM/SBR-NC nanocomposites. The EPDM/SBR nanocomposites developed by this research work could be effectively used in hose and gaskets.

## References


1. Franta I (1989) Elastomers and rubber compounding materials: manufacture, properties and applications. Elsevier, Amsterdam
2. Morton M (1999) Rubber technology. Springer Science BusinessMedia, Dordrecht
3. Heinrich G, Klüppel M, Vilgis TA (2002) Reinforcement of elastomers. Curr Opin Solid State Mater Sci 6(3):195–203
4. Mark JE, Erman B, Roland M (eds) (2013) The science and Technology of Rubber. Academic Press, UnitedStates
5. Ray SS, Okamoto M (2003) Polymer/layered silicate nanocomposites: are views from preparation to processing. Prog Polym Sci 28(11):1539–1641
6. Gopi JA, Patel SK, Chandra AK, Tripathy DK (2011) SBR-clay carbon black hybrid nanocomposites for tire tread application. J Polym Res 18(6):1625–1634
7. Karger Kocsis J, Wu CM (2004) Thermoset rubber/layered silicate nanocomposites. Status and future trends. Polym Eng Sci 44(6): 1083–1093
8. Ma J, Xiang P, Mai YW, Zhang LQ (2004) A novel approach to high performance elastomer by using clay. Macromol Rapid Commun 25(19):1692–1696
9. Monfared A, Jalali-Arani A (2015) Morphology and rheology of (styrene butadiene rubber/ acrylonitrile–butadiene rubber) blends filled with organo clay: the effect of nanoparticles localization. Appl Clay Sci 108:1–11
10. Nematollahi M, Jalali-Arani A, Golzar K (2014) Organo clay maleated natural rubber nanocomposite. Prediction of abrasion and mechanical properties by artificial neural network and adaptive neuro-fuzzy inference. Appl Clay Sci 97:187–199
11. Thomas S, Stephen R (2010) Rubber nanocomposites: preparation, properties and applications. John Wiley & Sons, Asia, pp 169–173
12. Zhang L, Wang Y, Wang Y, Sui Y, Yu D (2000) Morphology and mechanical properties of clay/styrene–butadiene rubber nanocomposites. J Appl Polym Sci 78(11):1873–1878
13. Pal K, Rajasekar R, Kang DJ, Zhang ZX, Pal SK, Das CK (2010) Effect of fillers on natural rubber/high styrene rubber blends with nano silica: morphology and wear. Mater Des 31:677–686
14. Mishra S, Shimpi NG, Patil UD (2007) Effect of nano $CaCO_3$ on thermal properties of styrene butadiene rubber (SBR). J Polym Res 14:449–459
15. Lorenz H, Fritzsche J, Das A, Stockelhuber KW, Jurk R, Heinrich G (2009) Advanced elastomer nano-composites based on CNT-hybrid filler systems. Compos Sci Technol 69:2135–2143
16. Gatos KG, Karger-Kocsis J (2005) Effects of primary and quaternary amine intercalants on the organo clay dispersion in a sulfur – cured EPDM rubber. Polymer 46(9):3069–3076
17. Zheng H, Zhang Y, Peng Z, Zhang Y (2004) Influence of clay modification on the structure and mechanical properties of EPDM/ montmorillonitenano composites. Polym Test 23(2):217–223
18. Ahmed S, Basfar AA, Aziz MA (2000) Comparison of thermal stability of sulfur, peroxide and radiation cured NBR and SBR vulcanizates. Polym Degrad Stab 67(2):319–323
19. Meneghetti P, Shaikh S, Qutubuddin S, Nazarenko S (2008) Synthesis and characterization of styrene–butadiene rubber - clay nanocomposites with enhanced mechanical and gas barrier properties. Rubber Chem Technol 81(5):821–841
20. Sadhu S, Bhowmick AK (2004) Preparation and properties of styrene–butadiene rubber based nanocomposites: the influence of the structural and processing parameters. J Appl Polym Sci 92(2): 698–709
21. Durandish M, Alipour A (2013) Investigation into morphology, microstructure and properties of SBR/EPDM/ organomontmorillonite nanocomposites. Chin J Polym Sci 31(4): 660–669
22. Naseri ASZ, Jalali-Arani A (2015) A comparison between the effects of gamma radiation and sulfur cure system on the micro structure and cross link network of (styrene butadiene rubber/ ethylene propylene diene monomer) blends in presence of nanoclay. Radiat Phys Chem 115:68–74
23. Bock J, Su SJ (1970) Interpretation of the Infrared Spectra of Fused Silica. J Am Ceram Soc 53:69–73
24. De Caillerie JB, De la Kermarec M, Clause O (1995) Si NMR observation of an amorphous magnesium silicate formed during impregnation of silica with mg (II) in aqueous solution. J Phys Chem 99:17273–17281
25. Hunt LP, Dismukes JP, Amick JA, Schei A, Larsen K (1984) Rice hulls as a raw material for producing silica. J Electrochem Soc 131: 1683–1686
26. Tinker AJ, Jones KP (1998) Blends of natural rubber, novel techniques for blending with speciality polymers. Chapman & Hall, London ISBN0–412–81940-6
27. Choi SS, Nah C, Lee SG, Joo CW (2003) Effect of filler–filler interaction on rheological behaviour of natural rubber compounds filled with both carbon black and silica. Polym Int 52(1):23–28
28. Muraleedharan Nair T, Kumaran MG, Unnikrishnan G (2004) Mechanical and aging properties of cross-linked ethylene propylene Diene rubber / styrene butadiene rubber blends. J Appl Polym Sci 93:2606–2621
29. Haloi DJ, Singha NK (2011) Synthesis of poly (2-ethylhexyl acrylate)/clay Nanocomposite by in situ living radical polymerization. J Polym Sci A Polym Chem 49:1564–1571
30. Datta H, Singha NK, Bhowmick AK (2008) Structure and properties of tailor-made poly(ethyl acrylate)/clay Nanocomposites prepared by in situ atom transfer radical polymerization. J Appl Polym Sci 108:2398–2407
31. Vishvanathperumal S, Gopalakannan S (2018) Effects of the Nanoclay and crosslinking systems on the mechanical properties of ethylene-propylene-diene monomer/styrene butadiene rubber blends Nanocomposite. Silicon 11(1):117–135
32. Ansarifar A, Azhar A, Ibrahim N, Shiah SF, Lawton JMD (2005) The use of a silanised silica filler to reinforce and crosslink natural rubber. Int J Adhes Adhes 25:77–86
33. Yu J, Gao YF, Guo ZX (2001) Grafting of polystyrene onto a nanometer silica surface by micro emulsion polymerization. Chin J Polym Sci 20:71–76
34. Zhu A, Cai A, Zhou W, Shi Z (2008) Effect of flexibility of grafted polymer on the morphology and property of nanosilica / PVC composites. Appl Surf Sci 254:3745–3752
35. Vaibhav V, Vijayalakshmi U, Mohana Roopan S (2015) Agricultural waste as a source for the production of silica nanoparticles. Spectrochim Acta Part A Mol Biomol Spectroscopy 139: 515–520
36. D15 ASTM (1958) Standard test method for rubber property-sample preparation for physical testing of rubber products. Annual Book of ASTM Standards, Philadelphia
37. Manoj KC, Kumari P, Rajesh C, Unnikrishnan G (2010) Aromatic liquid transport through filled EPDM/NBR blends. J Polym Res 17: 1–9

38. Sujith A, Unnikrishnan G (2006) Molecular sorption by heterogeneous natural rubber/ poly (ethylene-co-vinyl acetate) blend systems. J Polym Res 13:171–180
39. Thomas PC, Tomlal JE, Selvin TP, Thomas S, Joseph K (2010) High-performance nanocomposites based on acrylonitrile butadiene rubber with fillers of different particle size: mechanical and morphological studies. Polym Compos 31:1515–1524
40. Flory PJ, Rehner J (1943) Statistical mechanics of cross-linked polymer networks I. Rubber like elasticity. J Chem Phys 11:512
41. Naseri ASZ, Jalali-Arani A (2015) A comparison between the effects of gamma radiation and sulfur cure system onthe microstructure and crosslink network of (styrene butadiene rubber/ethylene propylene diene monomer) blends in presence of nanoclay. Radiat Phys Chem 115:68–74
42. Noriman NZ, Ismail H (2012) Properties of styrene butadienerubber (SBR)/ recycled acrylonitrile butadiene rubber (NBR) blends: the effects of carbon black/silica (CB/silica) hybrid filler and silane coupling agent, Si69. J Appl Polym Sci 124:19–27
43. Teh PL, MohdIshak ZA, Hashim AS, Karger-Kocsis J, Ishiaku US (2004) Effects of epoxidized natural rubber as a compatabilizer in melt compounded natural rubber-organo clay nanocomposites. Eur Polym J 40:2513–2521
44. Ismail H, Chia HH (1988) The effects of multifunctional additive and vulcanization systems on silica filled Epoxidized natural rubber compounds. Eur Polym J 34:1857–1863
45. Fu JF, Chen LY, Yang H, Zhong QD, Shi LY, Deng W (2012) Mechanical properties, chemical and aging resistance of natural rubber filled with nano-$Al_2O_3$. Polym Compos 33:404–411
46. Kueseng K, Jacob KI (2006) Natural rubber nanocomposites with SiC nanoparticles and carbon nanotubes. Eur Polym J 42:220–227
47. Wang QL, Yang FY, Yang QA, Chen JH, Guan HY (2010) Study on the mechanical properties of nano-Fe3O4 reinforced nitrile butadiene rubber. Mater Des 31:1023–1028
48. Xu D, Karger-Kocsis J, Major Z, Thomann R (2009) Unlubricated rolling wear of HNBR/FKM/MWCNT compounds against steel. J Appl Polym Sci 112:1461–1470
49. Vishvanathperumal S, Gopalakannan S (2017) Swelling Properties, Compression Set Behavior and Abrasion Resistance of Ethylene-propylene-diene Rubber/Styrene Butadiene Rubber Blend Nanocomposites. Polym Korea 41:433–442